Iraqi National Journal of Earth Science
www.earth.mosuljournals.com

Paleoenvironment and Paleoclimatic Imprints of the Khurmala Formation in Bakoz Village, Duhok Governorate, Northern Iraq

Ahmed N. Al-Fattah[1*], Zaid A. Malak [2], Ali Ismail Al-Juboury [3], Maha A. Al−Shammary [4]

[1,2,4] *Department of Geology, College of Science, University of Mosul, Mosul, Iraq.*
[3] *Petroleum Engineering Department, College of Engineering, Al-Kitab University, Kirkuk, Iraq.*

Article information

Received: 14- Apr -2024

Revised: 15- June -2024

Accepted: 19- Aug -2024

Available online: 01- Jan – 2025

Keywords:
Iraq, Duhok
Paleocene- Eocene
Paleoclimate
Tempestite
Khurmala formation

Correspondence:
Name: Ahmed N. Al-Fattah
Email: anf1277@uomosul.edu.iq

ABSTRACT

Although the deposition of the Khurmala Formation within the Paleocene-Eocene AP10 Megasequence was controlled by the tectonic environment, the synchronization of AP10 deposition with the so-called the Paleocene - Eocene thermal maximum extreme global climatic hyperthermal events had left an imprint on the details of the Khurmala Formation characteristics. The present study aims to elicit the depositional environment for Khurmala Formation, in addition to trace the inherited paleoclimatic indicators or imprints on the studied section. The study of litho-microfacies of the Khurmala Formation in the Bakoz village section in Dohuk City, northern Iraq reveals that the Khurmala Formation was deposited in a ramp paleoenvironment affected by storm action under warming tropical climate conditions. Planktonic foraminifera age determination in integration with both sedimentary environment properties and x-ray diffraction interpretations indicate that the deposition of the Khurmala Formation bears many imprints of long-term warming trend conditions from the Late Paleocene to Early Eocene (58 to 50 Ma).

DOI: 10.33899/earth.2024.148800.1269,

البيئة القديمة والبصمات المناخية القديمة لتكوين خورمالة في قرية باكوز، محافظة دهوك، شمالي العراق

أحمد نذير ذنون آل فتاح[1*]، زيد عبد الوهاب ملك[2]، علي اسماعيل عبد الله الجبوري[3]، مها عطيه الشمري[4]

[1،2،4]قسم علوم الأرض، كلية العلوم ، جامعة الموصل، الموصل، العراق.

[3] قسم هندسة النفط، كلية الهندسة، جامعة الكتاب، كركوك، العراق.

معلومات الارشفة

تاريخ الاستلام: 14- ابريل -2024

تاريخ المراجعة: 15- يونيو-2024

تاريخ القبول: 19- أغسطس-2024

تاريخ النشر الالكتروني: 01- يناير -2025

الكلمات المفتاحية:

العراق، دهوك

الباليوسين – الايوسين

المناخ القديم

رواسب العواصف

تكوين خورماله

المراسلة:

الاسم: أحمد نذير ذنون آل فتاح

Email: anf1277@uomosul.edu.iq

الملخص

على الرغم من أن ترسب تكوين خورمالة ضمن التعاقب الكبير لفترة الباليوسين-الإيوسين AP10 كان تحت سيطرة البيئة التكتونية، إلا أن تزامن ترسب ذلك التعاقب AP10 مع ما يدعى بالأحداث المناخية الحرارية العالمية المتطرفة بين عصري الباليوسين/الأيوسين (PETM) كان له بصمة واضحة على تفاصيل خصائص ذلك التكوين. تهدف الدراسة الحالية إلى استنباط البيئة الترسيبية لتكوين خورمالة، فضلا عن تتبع المؤشرات أو البصمات المناخية القديمة الموروثة في المقطع المدروس. اذ أظهرت دراسة السحنات الصخرية والسحنات الدقيقة لتكوين خورمالة في مقطع قرية باكوز في مدينة دهوك، شمالي العراق أن تكوين خورمالة قد ترسّب في بيئة الرصيف المنحدر القديمة المتأثرة باحداث العواصف البحرية تحت الظروف المناخية الاستوائية الدافئة. كما ان تحديد عمر الفورامنيفيرا الطافية بالتكامل مع كل من خصائص البيئة الرسوبية وتفسير النتائج المعدنية لحيود الأشعة السينية أشارت إلى أن ترسيب تكوين خورمالة قد تضمن العديد من بصمات ظروف المسار الحراري طويل الامد من العصر الباليوسيني المتأخر مرورا بالعصر الأيوسيني المبكر (58 إلى 50 مليون سنة).

DOI: 10.33899/earth.2024.148800.1269,

Introduction

Many previous studies dealt with sedimentological features of the Khurmala Formation and its paleoenvironment is represented by shallow marine environment distributed between the shoal-lagoons and tidal flat environments (Al-Banna *et al.*, 2006; Al-Dabagh, 2010; Salih, 2010; Salih, 2013; Asaad and Balaky, 2018; Barazani and Al-Qayim, 2019; Al-Hadeedy and Khalaf, 2020; Al-Qayim and Barazani, 2021; Asaad *et al.*, 2022).

Since the climate is considered an effective and important factor in any sedimentary environment, the linkage between the paleoenvironmental and paleoclimatic studies is a good step in the right trend. This concept is especially promoted when there are an exceptional and extreme paleoclimatic events as the Paleocene Eocene thermal maximum event (PETM).

The PETM is the most rapid global warming event known in Earth's history (Zamagni *et al.*, 2012). The envisaged close causal link between climate warming and tropical storms during the early Paleogene hyperthermal events (Jiang *et al.*, 2022) is the essential principle to investigate the Khurmala Formation as "coastal environment" creteria for paleoclimate

Although the deposition of the Khurmala Formation is synchronized with extreme paleoclimatic events between the Paleocene and the Eocene, previous studies did not clarify the paleoclimatic signals and role of paleoclimate on its depositional environment. Therefore, this

study aims to elicit the Khurmala Formation depositional environment as well as to trace the inherited paleoclimatic indicators or imprints of the formation at the studied section.

Geological Setting

The Khurmala Formation (Paleocene – Lower Eocene) was first described from well Kirkuk-114 by Bellen (Bellen, 1953 in Bellen *et al.*, 1959). Paleocene - Eocene sediments have attain a thickness of 1200 m, and condensed sediment accumulation rates were about 10-40 m/Ma (Aqrawi *et al.*, 2010). These sediments are part of the Paleocene–Eocene Megasequence AP10, which is subdivided into two sequences according to the regional unconformity at the base of the Middle Eocene: The Paleocene–Early Eocene (In which the Kolosh and Sinjar / Khurmala formations were deposited) and Middle–Late Eocene sequences (Gercus/Avanah and Pila Spi formations) (Fig.1).

The Paleocene–Eocene Megasequence AP10 was deposited during a period of renewed subduction and volcanic arc activity associated with the final closure of the Neo-Tethys. This led to an uplift along the NE margin of the Arabian Plate with the formation of ridges and basins generally of NW-SE trend in N and Central Iraq and EW trend in W Iraq (Jassim and Buday, 2006).

The Khurmala Formation was most deposited in a relict basin analogous to the southeast part of the Kolosh trough. This basin was separated from the offshore Aaliji basin by a partly disconnected submarine ridge on which shoals of Sinjar Formation (Jassim and Goff, 2006). The inefficiency of the islands and shoals to separate the lagoon from the open sea, and the continuous changing of islands position, shoals and reef knolls in the shoal belt and the lagoon resulted in a great degree of vertical and horizontal variability of the sedimentation during this period (Bellen *et al.*, 1959). The carbonates (Khurmala Formation) have been interfingered with the clastics sediments (Kolosh Formation) at Bekhme Gorge (Malak, 2011), and in Duhok and Shaqlawa areas (Karim, 2009).

The present study deals with an outcrop of the Kolosh -Khurmala formations of about 11 m thick located in the northern limb of the Bekhair Anticline, near Bakoz village, Duhok City approximately at Lat. 36° 55' 50" N and Long. 43° 00' 57" E (Fig.2).

Bekhair Anticline is located within the Unstable Shelf, the High Folded Zone. It is asymmetrical double plunging anticline trending NW – SE and extending about 72 Km from Zawita/Besari area (the southeastern plunge) to the Deraboon village near the Iraqi− Syrian-Turkish border (the northwest plunge) (Al-Azzawi and Al-Hubaiti, 2009).

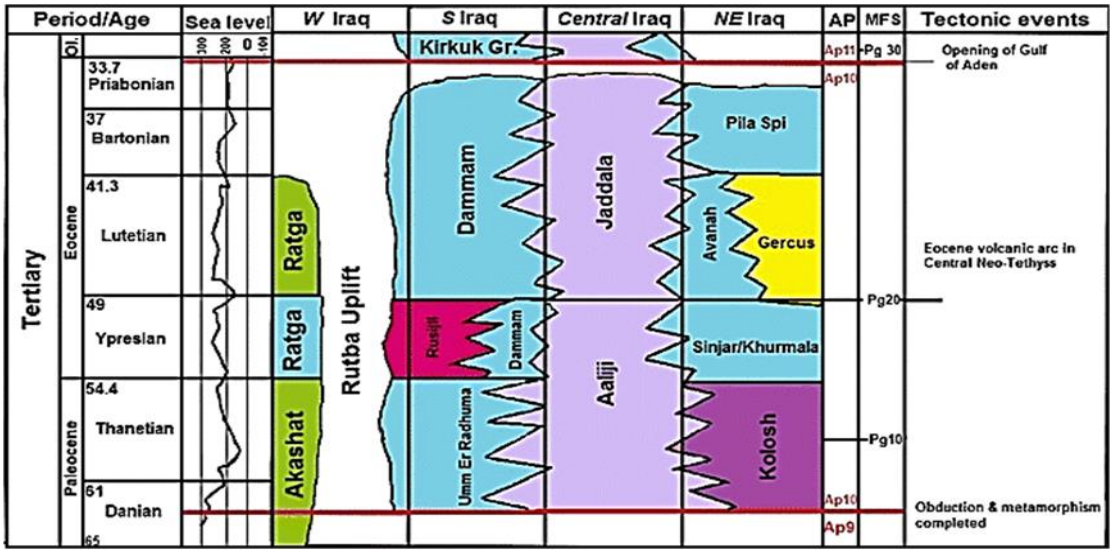

Fig. 1. Megasequence (AP10) in the eastern, central and western Iraq (after Jassim and Buday, 2006)

Materials And Methods

The study focuses on a detailed field lithological description. More than 30 samples were collected from the surface section at every change in lithology and physical properties. A detailed description of more than 25 thin sections is performed using a polarized microscope. Dunham's (1962) and Embry and Klovan (1971) classifications are used to classify the donated microfacies. The Ramp mirofacies (RMF) and facies Zone (FZ) of Wilson (1975) and Flügel (2004, 2010) are used as much as possible for comparison. The litho-microfacies evidence is used to identify and determine the depositional environment of the formation.

The obtained planktonic foraminifera samples from the uppermost part of the Kolosh Formation rocks enabled us to identify the Paleocene/Eocene chrono-boundary index species at the studied section according to Berggren and Pearson (2005). This makes it faster and easier to characterize the PETM paleoclimatic event position and later search for other indicators based on the other features.

X-ray diffraction (XRD) analysis is performed at the Premier Laboratory in Houston, USA on bulk rock shale samples using a Bruker D8 Advance XRD instrument. Mineral phase quantification in the bulk diffraction pattern is accomplished using the TOPAS software package.

Lithostratigraphy

Khurmala Formation overlies the Kolosh Formation mostly with a sharp contact estimated at the last appearance of silty claystone of the Kolosh Formation which is capped by an intraformational conglomerate of the Khurmala Formation (50 cm thick) which is also noticed by Znad and Aljumaily (2019). Whereas the upper contact of the formation is conformable and gradational with the overlaying Gercus Formation.

Khurmala Formation consists of three different thickness cycles (Fig. 3): the first cycle is composed of 50 cm thick intraformational conglomerate (calcrudite) at the lower contact with Kolosh Formation. The pebbles (carbonate and some chert) are about 0.4 to 2.5 cm in size, rounded, and surrounded by the carbonate matrix overlain by 45 cm thick of well-bedded, hard, dense, and white to creamy limestone ended by a rich larger fauna (pelecypods) followed by a thin bed of friable, black–grey shale (45 cm. thick) intercalated by two thin beds (10 cm thick) of fossiliferous limestone. The first cycle capped by 70 cm thick friable black shale.

The second cycle begins with 5 m thick of hard, white - creamy limestone bed. Dissolved vugs are present in the middle part of this bed. This bed is capped by (150 cm thick) grey – greenish friable shale. The last cycle has numerous changes at every foot, beginning with (160 cm) carbonate sandstone that had small lime gravels (2 cm in size) at the base. Hummocky cross stratification (HCS) is present in the middle and upper divisions followed by 70 cm thick alternative laminated carbonate sandstone and siltstone. *Thallasinoid* bioturbation with horizontal arrangement is present in the upper part of the cycle. The upper contact of the formation with the overlaying Gercus Formation (red siliciclastic deposits) seems to be gradational (Fig. 3).

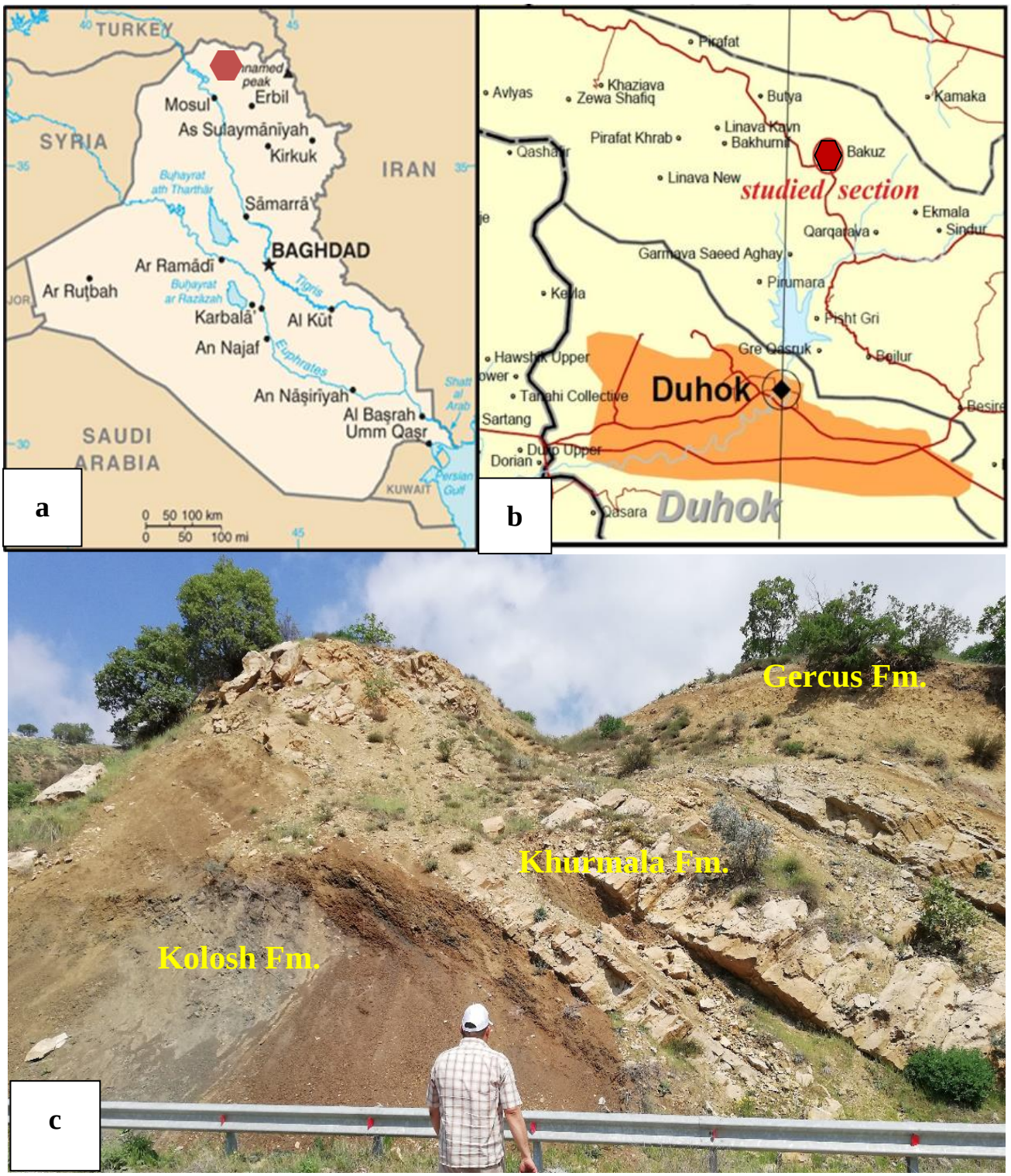

Fig. 2. a: Location map of Iraq, b: location map of the studied section in Duhok City, c: Field image showing the succession of the Khurmala Formation at Bakoz village.

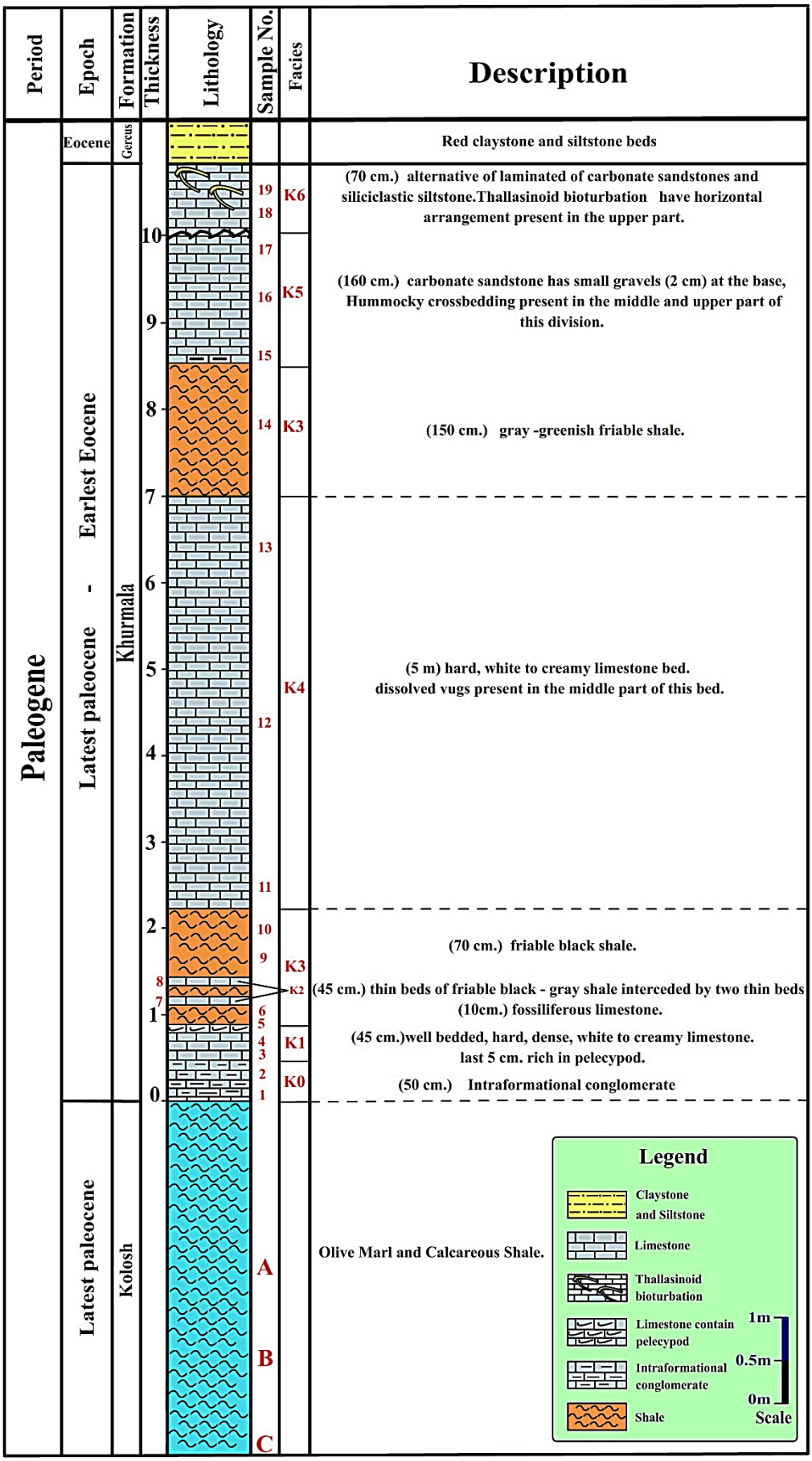

Fig. 3. Lithological description and litho- microfacies of the studied section.

Result and Discussion

Lithofacies and microfacies analysis

After detailed field and microscopic study, we can identify the following lithofacies and microfacies (Fig. 3) summarized as follows:

1- Intraformational conglomerate lithofacies (K0)

It is about 90 cm thick which occurs at the lower part of the Khurmala Formation (Fig. 4). It includes different sizes, random distribution of carbonate gravels and some extraclast embedded within the carbonate matrix (matrix supported). The gravel diameter is up to 2.5 cm, badly sorted, and ovoid in shape. The last 10 cms contain macrofossils (Pelecypoda) with scattered pebbles. This lithofacies resembles floatstone; the ramp facies zone (RMF9) and (RMF7) of Flügel (2010).

Interpretation

The sedimentological evidence refers to deposition in an open inner ramp to the proximal mid-ramp environment (Flügel, 2010).

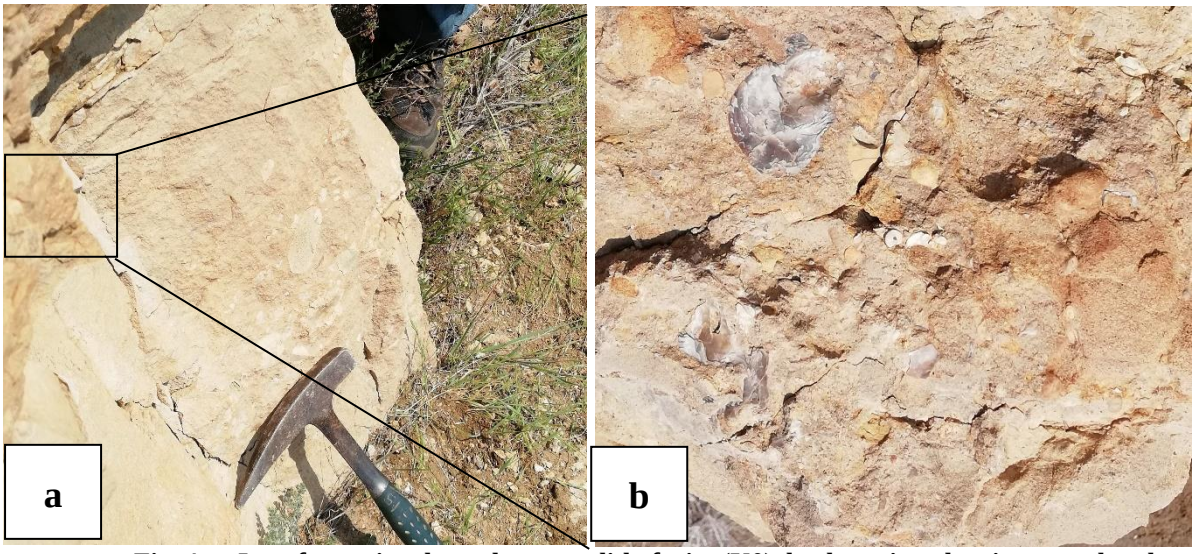

Fig. 4. a. Intraformational conglomerate lithofacies (K0). b. close view showing gravel and macrofossils shell.

2- Bioclastic lime wackestone / packstone microfacies (K1)

This microfacies consists of hard and well-bedded (0.1 – 0.8 m. thick) limestone. The allochems reach 50% of the total content and sometimes exceed the limit 80%, especially at the lower part of the formation (Fig. 5 a). They include benthonic foraminifera (*Rotalids*, *Quenqueloculina* sp.), blue-green algae, echinoderm, ostracod and pelecypods bioclasts, in addition to some intraclast and extraclasts (Qtz grains). The matrix is composed of micrite and microspar. Dissolution, dolomitization and recrystallization are present.

Interpretation

The presence of bioclasts indicates a deposition in low to moderate energy that developed in protected shallow subtidal environments (less th,an 30 m depth) reflecting the inner shelf \ ramp depositional environments indicated by abundant carbonate mud and the presence of miliolids (Bathurst, 1975; Al-Ameri and Lawa, 1986; Di Stefano and Ruberti, 2000). This microfacies may be affected by offshore storm surges that transport some intraclast and extraclasts (Qtz grains). It most probably resembles RMF28, and RMF26 that was deposited in carbonate sand shoals and banks (Flugel, 2010).

3- Pelecypodal lime wackestone microfacies (K2)

This microfacies is recorded only in a bed near the lower contact of the Khurmala Formation, which appeared as a thin bed (10-15 cm. thick) of hard, milky limestone. It is composed of pelecypod shells (35%), in addition to the small amount of Rotalid test (2.5-5%), bioclasts (3%) and extraclast (1%), embedded in micrite crystals forming the matrix (Fig. 5 b).

Interpretation

The bivalves prefer different sub−environments comprising the standard facies zones FZ 4, 5, 7 and 8 (Flügel, 2010). Shell concentrations can be formed by various processes (Kidwell, 1991). Event concentrations originate from short-term events, e.g., storm deposits (Flügel, 2010). Abundance pelecypod shells accumulation is usually limited within a shallow marine water (up to 40 m water depth) (Flügel, 2010), and the deposition of sediments might not have taken place in a restricted environment. These evidences point together to deposition in a shallow water, warm, tropical to sub-tropical marine environment beside the land in changeable conditions and being affected by episodic sea storms or low tides such as lagoon and back reef connected to the open sea (Sharma and Patnaik, 2010, 2013a, b; Tucker *et al.,* 1990). So, this microfacies is compared with the SMF 12, FZ 8, and RMF 20 of Wilson (1975) and Flügel (2004, 2010).

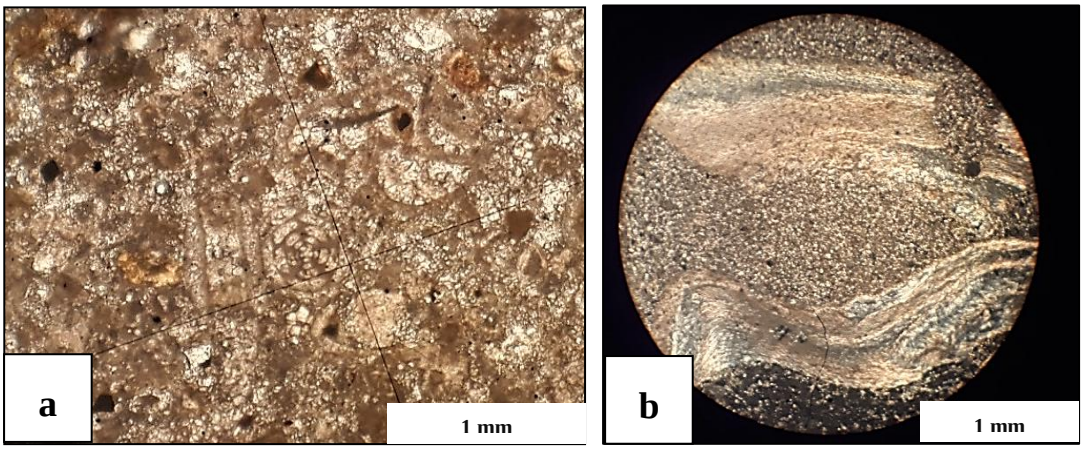

Fig.5. a. Bioclastic lime wackestone / packstone microfacies (K1); b. Pelecypodal lime wackestone microfacies (K2).

4- Marl Lithofacies (K3)

This lithofacies (about 45 cm to 1.5 m thick) consists of brown to light grey friable Marl. It appears at the lower part of the formation (45 – 70 cm) interbedded with white–yellow hard limestone without any internal structure and fossils. The same lithofacies reappears at the upper part of the formation (1.5 cm thick) as light grey friable marl (Fig. 6 a).

Interpretation

This lithofacies represents a clastic influx driven from the land neighboring coastal environment according to the absence of marine fossils. Deposition of fine particles (clay) demands deposition from suspension in quite water (Chen *et al.,* 2011). The dominance of clay material in this microfacies may attributed to its deposition during times of high terrestrial input and/or depression of carbonate production (Chen *et al.,* 2011; Myrow *et al.,* 2012; Myrow *et al.,* 2015). This lithofacies may compared with the RMF19.

5- Dolomitic lime mudstone/ wackestone microfacies (K4)

This microfacies appeared at the middle part of the formation (5m thick) as milky, massive, and vuggy hard dolomitic limestone (Fig. 6 b). Severe dolomitization of micrite has produced micro-textured suture mosaic and sieve mosaic dolomite. According to Randazzo and Zachos (1984), the homogenous dolomitization of mudstone yields micro-textured sutured

mosaic wherever there is dissolution of allochems; similarly, the wackestone generally is dolomitized to micro-texture sieve mosaic. Therefore, the dolomite in the Khurmala Formation reflects the fabric of original lime mudstone - wackestone microfacies.

Interpretation

These types of microfacies may accumulate in pools of very shallow subtidal to intertidal environments. These microfacies could be compared with the SMF21 (RMF 22 peritidal) within FZ-8 (Wilson, 1975 and Flugel, 2010).

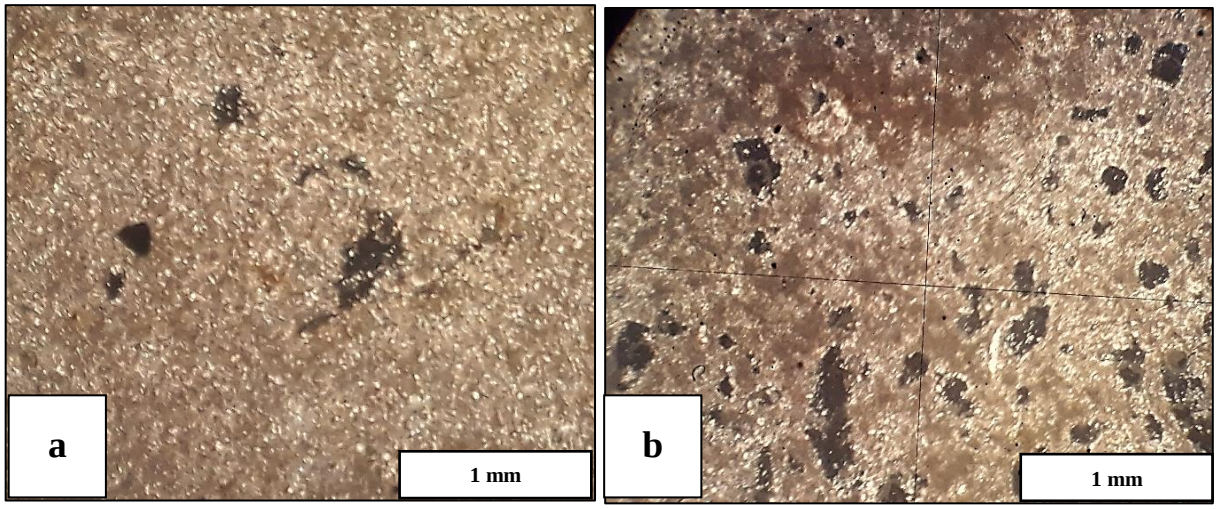

Fig.6. a Marl Lithofacies (K3). b. Dolomitic lime mudstone/ wackestone microfacies (K4)

6- Hummocky cross-stratification (HCS) - Parallel lamination calcarenitic Lithofacies (K5)

It is generally whitish to milky bed (160 cm thick) composed of grains (fine to coarse) carbonate sand, rounded to subrounded in shape, with low angle hummocky cross-stratification at the lower and middle part of the bed and parallel lamination at the top (Fig. 7 a b). The petrographic analysis shows intraclasts (70%) and extraclasts (25%) of siliciclastic, chert and quartz rock fragments surrounded by carbonate micrite.

Interpretation

The presence of hummocky cross-stratification indicates traction transport and deposition under the effect of unidirectional and volatility flows of variable severity or deposition from powerful storm-generated waves (Myrow and Southard, 1991, 1996; Dumas *et al.*, 2005). Parallel lamination in beds with hummocky cross-stratification indicates a high current regime during the deposition of the tempestite especially in the intertidal zone (Flugel, 2010).

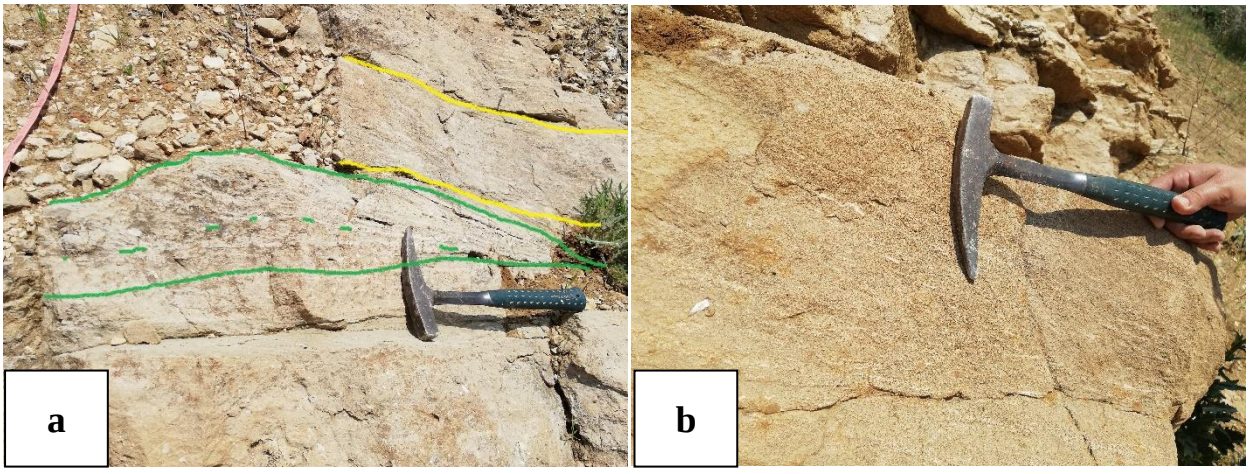

Fig. 7. a. Hummocky cross-stratification (HCS), b. Parallel lamination calcarenite lithofacies (K5)

7- Calcisiltite / Marl Lithofacies (K 6)

It is about 70 cm thick, brown-grey in color, composed of marl and siltstone alternation, located above the HCS - Parallel lamination calcarenite facies. It displays *Thalassinoides* burrows and lamination (Figure 8 a and b).

Interpretation

Bioturbated beds refer to spells of decline energy and colonization by infaunal organisms in a shallow-marine environment (Myrow *et al.,* 2015). The fine grains and good sorting in these facies suggest the deposition in a low-energy environment, most likely in shoreline setting depending on the abundance of bioturbation and quartz. These advantages are coherent with a lower shoreface environment that offers as a transition zone where terrestrial-derived quartz sand is mixed with offshore carbonate. Bioturbation is common in these transition zones because the sediment is less frequently mobilized than laminated sediment reworked by marine currents and waves at the upper shoreface (Myrow *et al.*, 2015).

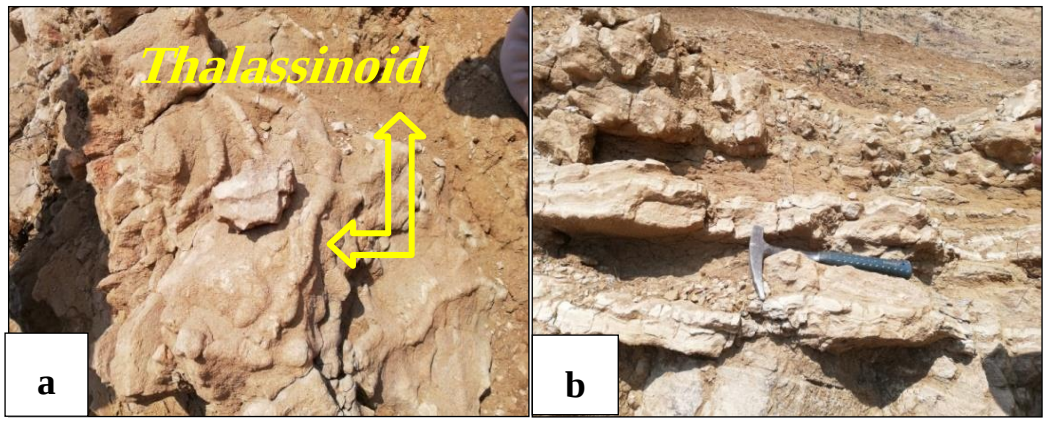

Fig. 8. Field photograph of Calcisiltite / Marl Lithofacies (K6); showing a) the *Thalassinoides* burrows; b) lamination.

Paleontological evidence

To diagnose the lithosomes influenced by the PETM extreme climatic event is necessary to trace the Paleocene / Eocene epochs boundary. This is accomplished by studying and identifying the planktonic foraminifera in three samples of marl and/or calcareous shale within the uppermost part of the Kolosh Formation, nearest the lower contact with the Khurmala Formation. These samples are A, B, and C; the A sample is located 2 meters under the lower contact of the Khurmala Formation, and the others are located downwards to the Kolosh Formation with a sampling distance of 1 meter. The deposits between the lower contact of the Khurmala Formation and sample A did not contain planktonic foraminifera. A group of species belonging to planktonic foraminifera has been identified as shown below (Fig. 9).

1. Sample (A) includes the following group of planktonic foraminifera: Globanomalina pseudomenadii, Globanomalina enrenbergi, Morozovella acuta, Acarinina nitida, Morozovella conicotruncana, and Morozovella Velascoensis

2. Sample (B) comprises the following group of planktonic foraminifera: Subbotina triloculinoides, Acarinina nitida, Morozovella Velascoensis, and Morozovella conicotruncana.

3. Sample (C) contains the following group of planktonic foraminifera: Preamurica inconstan, Parasubbotina pseudobilloids, Preamurica uncinata, Morozovella praecursoria, Morozovella angulata,and Morozovella primitiva.

Based on the groups of the identified planktonic foraminifera, it appears that the group of foraminifera in the C sample usually indicates the age (early to middle Selandian). On the other hand, the presence of the planktonic foraminifera diagnosed in the A and B samples indicates late Selandian to late Thanetian age within the P4-P5 (Berggren *et al.*, 1995; Berggren and Norris, 2003; Berggren and Ouda, 2003; Orabi and Hassan, 2015; Abdulsamad, 2017). This means that sample A represents the latest Paleocene, and the next deposits (Khurmala Formation) were deposited in the latest Paleocene and continued to Eocene. In other words, the Khurmala Formation was necessarily influenced by PETM climatic events.

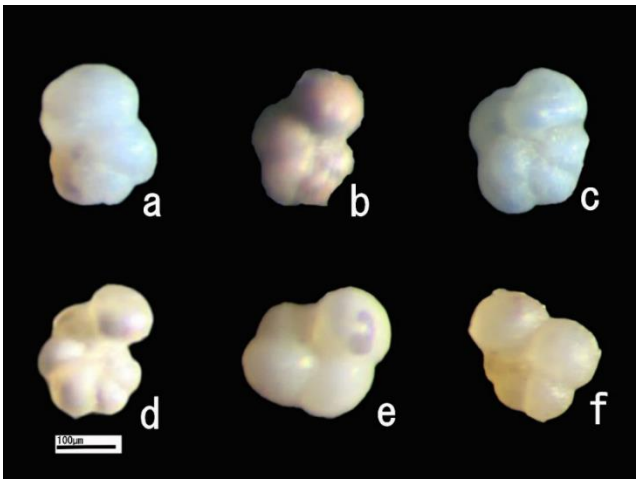

Fig. 9. a) Parasubbotina pseudobilloids. b) Preamurica uncinate. c) Morozovella angulate. d) Morozovella praecursoria. e) Morozovella primitive. f) Preamurica inconstan.

Depositional environment

Based on the results of the facies analysis, the best environmental model of the Khurmala Formation in the current studied section is the carbonate ramp affected by storm action under warming tropical climate conditions as shown in Figure (10). The facies analysis of ancient storm deposits requires the integration of lithofacies and microfacies as mentioned by Flügel (2010).

Khurmala Formation begins with intraformational conglomerate bed (lithofacies K0). This lithofacies may be deposited during highstand (Al-Khalaif and Al- Mutwali, 2020) where the ramp was evolved to a shallow-water storm-influenced ramp evidenced by erosional sharp basal contacts between calcarenites and lime mudstones (Khurmala's lower contact). This led to the shedding of shoreface sediments into the offshore mid-ramp and the progradation of shallow-water sediments. The strong marine currents that are usually produced by storm waves can reach and erode newly semi-consolidated carbonate deposits, which are then redeposited as intraformational conglomerates (Eren *et al.*, 2002)

The Bioclastic lime wackestone/packstone microfacies (K1) and Pelecypodal lime wackestone microfacies (K2) facies are usually developed in restricted shallow marine environments as a back shoal or lagoon within an inner ramp characterized by medium energy condition, 30-40 meters water depth and medium to relatively high salinity due to the presence of miliolid. The presence of mollusks Bivalve also indicates a shallow marine environment and warm tropical to subtropical climate. This environment is usually found near the coast and affected by sea storms or low tides as represented by the lagoon environment (Bassi *et al.*, 2015).

The Dolomitic lime mudstone/wackestone microfacies (K4) and marl lithofacies (K3) alternation reflects a fluctuation in the environmental conditions within the inner ramp between subtidal (lagoon below fair-weather wave base) (K3) and shallow subtidal- intertidal (K4). The marl lithofacies (K3) is characterized by the absence of marine fossils indicating its proximity to the coastline, it was usually deposited in a calm water marine environment suitable for the deposition of clay grains transported from the neighboring land to the coastal environment

during and following storms, when rivers in flood debouched into the basin. The marl lithofacies is alternate in appearing with the carbonate beds in periods when the influx of clastic sediments from the land is low (Markello and Read, 1981)

The lithofacies HCS - Parallel lamination calcarenite (carbonate sandstones) (K5) usually indicates a deposition near the shoreline environment under the influence of sea waves (Einsele, 2000). The presence of Hummocky cross stratification (HCS) reflects its formation by storm wave-driven processes in the upper shoreface-foreshore or landward inner ramp. Such a sedimentary structure is usually found in many marine environments including tidal environments (Boersma and Terwindt, 1981; Tintiri, 2011).

The Khurmala Formation is enclosed by the calcisiltite / marl lithofacies (K6), which is characterized by the prevalence of trace fossils at the top of the succession as final facies indicating breaks in storm activity (Flügel, 2010). The mixture of carbonate /siliciclastic deposites represents the coastal marine sediments brought from nearby environments including the delta environment (Mutti *et al.,* 1984, 1985; Hallock and Glenn, 2006). These deposits are part of the clastic transition zone (lower shoreface) that usually encloses the Khurmala Formation and at the same time announcing the deposition of the Gercus Formation (maybe wave-dominated delta front environment) that is located directly above it in the Bakoz section (Figure. 10).

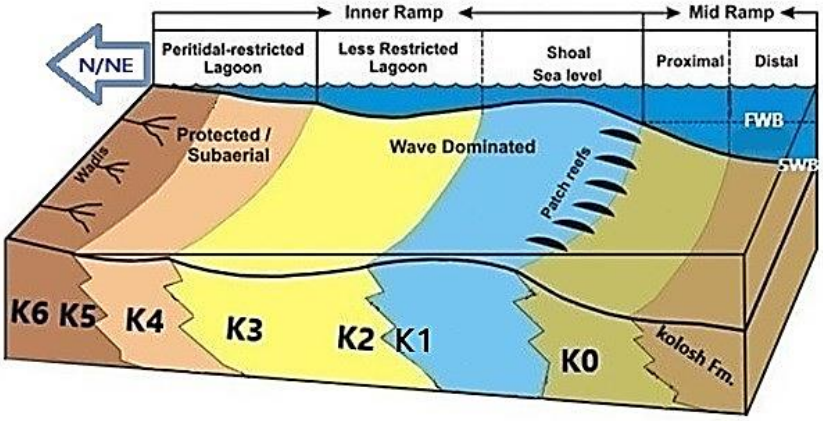

Fig. 10. The Depositional model of the Khurmala Formation in Bakoz Village. Modified from Abdulsamad et al. (2021). FWB: fair-weather wave base, SWB: storm wave base

Paleoclimatic indicators

Because of dolomitization and recrystallization, the Khurmala Formation age was given as Paleocene –E. Eocene adopt to its stratigraphic position (Jassim and Goff, 2006). Therefore, the presence of *Morozovella acuta and Morozovella Velascoensis* at the underlying Kolosh Formation (sample A) determines the end of the Paleocene age as mentioned above. Based on this, we proposed that the next rock of the Khurmala Formation could be deposited with the onset or after a brief time of the early Eocene, at least in the studied section. Thus, the proven age before litho contact position between two formations coincided with what was called the Paleocene Eocene thermal maximum (PETM) extreme global warming events, especially after documenting the absence of planktonic foraminifera between sample A and the first Khurmala beds, which are attributed to first planktonic dissolution interval (Arenillas and Molina, 2000 in Zili *et al.,* 2009) (El-Nady, 2005). Then, we can conclude that the next beds of the Khurmala Formation necessarily experienced the PETM event paleoenvironmental conditions as shown by the other following criteria.

The field indicators are readily visible in the uppermost part of the Kolosh Formation (Earliest Eocene), particularly after the beds that contain *morozovella* sample (A) (Latest Paleocene). These indicators as mentioned by Al-Fattah et al. (2020) are: the yellowish Tobacco colour of rocks, sharp facies change from clastic facies (Kolosh Formation) to dolomitic limestone facies (Khurmala Formation.) (Fig.2 c), and the presence of calcrudite (intraformational conglomerate lithofacies K0) followed by calcarenite tempestite at the first

limestone Khurmala Formation beds (microfacies K1, and mainly in microfacies K2). Furthermore, hummocky cross-stratification (lithofacies K5) as a unique noticed sedimentary structure indicating storm tempestite possibly induced by the later (early Eocene) phase of the event.

Facies interpretations were employed in the context of paleoclimate interpretation, particularly after identifying the strong relation of storm-induced deposits (Tempestite or eventstone) with Khurmala facies K0, K1 and K2, which are used as a function to paleoclimate (Flügel, 2010). These carbonate tempestite facies exclusively deposited under influence warming driven-storm condition, which coincides with an extreme PETM warming event. In other words, the Khurmala Tempestite facies was deposited by extreme warming PETM events driven- extreme strong storm may be reached to peritidal positions. So, the most likely interpretation for tidal flat HCS formation in shallow, nearshore environments is the extremely powerful storm surges are caused by PETM exceptional hyperthermal events.

Although dolomitization is diagenetic process that follows deposition and happened under different conditions, strong storms accompanied by heavy rain may enhance the later dolomitization in tidal flat environments (Bourrouilh-Le Jan, 1979).

Clay minerals are also used to support the concluded paleoclimatic interpretations (Table 1 and Fig. 11). The Tethyan Sea clays imprint remained in deposits during Tertiary age (Bolle and Adatte, 2001). The authigenic origin of clay minerals during PETM was low (Potter *et al.,* 2005). Montmorillonite is one of the smectite group minerals due to its authigenic phase being in reverse relation and competition with dolomite, the transported origin is more probable (Bristow *et al.,* 2012). Thus, the montmorillonite in the Khurmala Formation may be of detrital origin. Kaolinite mineral, on the other hand, is itself considered as a clue to the PETM events where the kaolinite pulse was used as a tool to determine the PETM events. This pulse suggested a high erosion rate as evidenced by the quartz ratio around and beyond the P/E boundary. Since kaolinite formation requires (1-2 m.y), its accumulation refers to transported origin to consistent with the high erosion rate during the short time of PETM event (170 k.y) (Zachos *et al.,* 1993; Röhl *et al.,* 2007; Harding *et al.,* 2011; Kemp *et al.,* 2016; Zeebe and Lourens, 2019; Tateo, 2020).

Both montmorillonite and kaolinite minerals accumulate under humid (rainy), warm and sometimes seasonality conditions (Dianto *et al.,* 2019; Bolle *et al.,* 2000). Table (1) shows increases in the kaolinite/montmorillonite ratio especially in sample A, which is compatible and coordinated with the fossils result, as well as in sample 12, which may be interpreted as another phase of the PETM, where this ratio is considered a strong clue for the PETM events (Tateo, 2020).

The common occurrence of albite mineral (more than 5%) especially after the P/E boundary in mixed siliciclastic/carbonate deposits (the uppermost Kolosh Formation) and later in the Khurmala Formation (samples 11-13) suggests its authigenic origin and confirms the extreme warming events (Zhang *et al.,* 2010; Wu *et al.,* 2022). While, Abeuov et al. (2023) pointed out that the abundance of muscovite in Paleocene-Eocene strata has been observed in previous studies and inferred to be detrital in origin and accumulates at areas with amplified current velocities such as shallowing. The probable relationship between muscovite abundance (Table 1) and high energy environmental conditions supports the facies interpretation of tempestite at the first Khurmala beds (facies K0, K1, and K2).

Calculation of kaolinite/muscovite as a paleoclimatic indicator shows variations interpreted as several short hyperthermals around the Paleocene-early Eocene, where the levels of high Kln/Ms (more than 1.1) (Table 1) interpreted as warming-wet periods that triggered intense chemical weathering (Do campo *et al.,* 2018). Mackenzie et al. (2018) suggests that the calcite -dolomite seas are characterized by elevated atmospheric CO_2 and are consistent with

the PETM event, and this is obvious in table (1). Finally, the occurrence of pyrite (sample A) may indicate anoxic conditions as an additional indicator (Al-Fattah *et al.*, 2020).

Table 1: X-ray diffraction mineral results in percent; yellow background refers to Khurmala Formation., light green background refers to Kolosh Formation., K/M=Kaolinite/Montmorillonite, K/Msv= Kaolinite/Muscovite, red line refers to Paleocene/Eocene contact.

Age	Sample No.	Quartz (%)	Albite (%)	Calcite (%)	Dolomite (%)	Muscovite (%)	Kaolinite (%)	Montmorillonite (%)	Gypsum (%)	Pyrite (%)	K/M	K/Msv
	13	17.82	5.21	1.39	19.65	21.24	20.22	14.47	–	–	1.397374	0.951977
	12	16.1	5.6	2.37	21.95	17.86	23.15	12.97	–	–	1.784888	1.296193
	11	11.5	6.27	12.15	18.25	15.45	20.61	15.79	–	–	1.305256	1.333981
	6	23.09	7.79	–	–	19.7	28	21.42	–	–	1.30719	1.42132
EOCENE	4	20.31	8.35	2.38	0.45	28.96	26.08	13.46	–	–	1.937593	0.900552
PALEOCENE	A	20.02	5.21	2.96	4.25	23.54	27.92	13.33	0.68	2.09	2.094524	1.186066
	B	18.69	2.71	16.35	16.06	11.6	18.76	15.83	–	–	1.185092	1.617241
	C	17.01	3.85	14.95	16.05	10.87	19.14	18.12	–	–	1.056291	1.76081

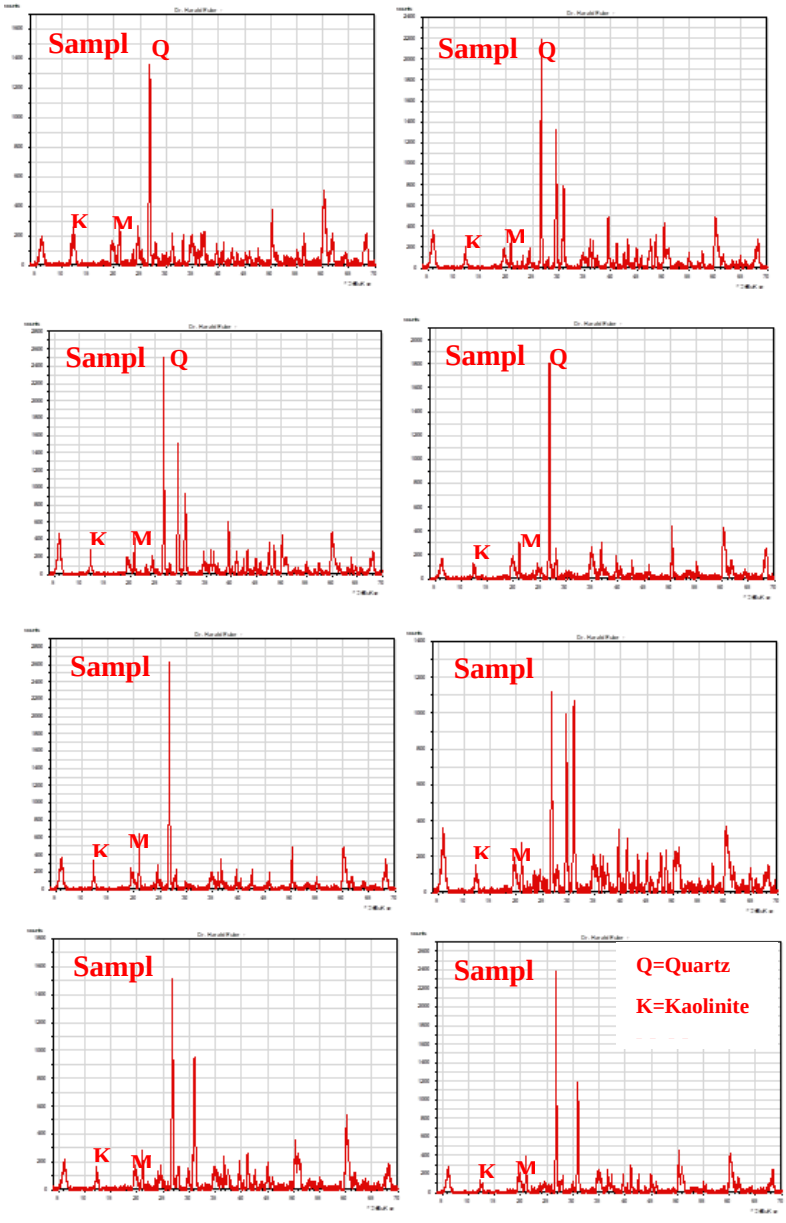

Fig. 11. XRD diffractogram patterns of selected samples.

Conclusion

1- The Khurmala Formation was undoubtedly influenced by Paleocene Eocene Thermal Maximum (PETM) or Early Eocene hyperthermal paleoenvironmental conditions as inferred by its stratigraphic position and paleontological criteria.

2- The environmental model of Khurmala Formation in the studied section is a carbonate ramp affected by storm action under warming tropical climate conditions.

3- Since Khurmala Formation represents the highstand system tract, transgressive systems tract (TST) and maximum flooding surface (MFS) had happened before the Khurmala Formation at the uppermost Kolosh Formation. This confirms the sea level rise associated with PETM and coincides with the paleontological results.

4- The carbonate tempestite facies (eventstone) of Khurmala Formation may be strongly related with the PETM exceptional warming-driven storm events.

5- Montmorillonite and kaolinite minerals have been accumulated from detrital sources under humid (rainy), warm and sometimes seasonal conditions supporting other paleoclimate evidences.

6- All paleoclimatic evidences or imprints of the Khurmala Formation can be attributed to the long-term warming trend from the Late Paleocene passing to the Early Eocene (58 to 50 Ma).

Acknowledgements

We express our thanks and appreciation to the College of Science and the University of Mosul for the facilities provided. We would also like to thank and appreciate Mr. Ezzat Ibrahim for participation in the fieldwork. Finally, we present our sincere thanks to the respected chief of the journal's editorial board, reviewers and editorial board members for their great efforts and valuable feedback.

References

Abdulsamad, E. O.; Tmallab, A. F. and Bu-Argoubc, F. M., 2017. Biostratigraphy of Palaeocene to Miocene foraminifera in concession 65, SE sirt basin, libya. libyan journal of science and technology. 9 (1), 46-52.

Abdulsamad, E. O.; Emhanna, S. A., Tawati, I. M., Khalifa, A. K., Fergani, R. S., Elhassi, M. F., Abdella, M. M., Elshari, A. S. and Eljawhari, A. H., 2021. Facies and stratigraphic architecture of "middle" Miocene carbonate succession at Al Jaghbūb Oasis, Northeastern Libya. Mediterranean Geoscience Reviews. 3, 431–454.

Abeuov, A., Dillinger, A. and Chanvry, A., Mathews, G., 2023. The abundance of detrital muscovite in Paleocene-Eocene uraniferous strata sheds a new light on paleo-drainage system, Chu Sarisu Basin, southern Kazakhstan, Conference paper.

Al-Ameri, T. and Lawa, F., 1986. Paleoecological and faunal interaction within Aqra limestone formation (N-Iraq). journal of the geological society of iraq, 19, 7–27.

Al-Azzawi, N.K.B., Al-Hubiti, S., T., 2009. The Fold Style Variations of Baikher Anticline - Northern Iraq, Iraqi Journal of Earth Sciences, Vol. 9, No. 1, pp. 1– 20,

Al-Banna NY, Al-Mutwali M.M, Al-Ghrear JS, 2006. Facies analysis and depositional environment of Khurmala Formation in Bekhair anticline –Duhok Area, North Iraq. Iraqi Jour Earth Sci 6(2):13–22.

Al-Dabagh, M.M., 2010. Facies and Depositional Model of Khurmala Formation (Paleocene-Early Eocene) At Selected Exposures from Northern Iraq. Unpublished M.Sc. Thesis, Mosul University, Iraq (In Arabic),114.

Al-Fattah, A. N., Al-Juboury, A.I., Ghafor, I. M., 2020. Paleocene-Eocene Thermal Maximum Record of Northern Iraq: Multidisciplinary Indicators and an Environmental Scenario. Jordan Journal of Earth and Environmental Sciences, 11 (2), pp. 126 – 145.

Al-Hadeedy, M. A. and Khalaf, S. K., 2020. Paleoenvironmental Study of Khurmala Formation by Ostracoda in Shaqlawa and Dohuk area, Northern Iraq, Iraqi Journal of Earth Sciences, Vol. 20, No. 2, pp. 148– 164. (In Arabic).

Al-Khalaif, S. S. M. and Al- Mutwali, M. M., 2020. Biostratigraphy and Sequence Stratigraphy and Depositional Environment of Kolosh Formation in Dohuk Area, Northern Iraq, Iraqi Journal of Earth Sciences, Vol. 20, No. 2, pp. 18–42. (In Arabic).

Al-Qayim, B., Barzani, A., 2021. Facies and stratigraphic associations of Sinjar and Khurmala Formation, Dohuk Area, Kurdistan Region, Iraq. Arabian Journal of Geosciences, 14 (3),165.

Aqrawi, A. A. M., Goff, J. C., Horbury, A.D. and Sadooni, F.N., 2010. The Petroleum Geology of Iraq: Scientific Press, 424 pp.

Arenillas, I., Molina, E., 2000, Reconstrucción paleoambiental con foraminíferos planctónicos y cronoestratigrafía del tránsito Paleoceno-Eoceno de Zumaya (Guipúzcoa): Revista Española de Micropaleontología, 32, 283-300.

Asaad, I. S., AL-Haj, M.A., Malak, Z. A., 2022. Depositional Setting of Khurmala Formation (Paleocene-Early Eocene) in Nerwa section, Berat Anticline, Kurdistan Region, Northern Iraq. Iraqi Geological Journal, 55 (IF), 20-39pp.

Asaad, I. S. and Balaky, S. M., 2018. Microfacies analysis and depositional environment of Khurmala Formation (Paleocene – lower Eocene), in the Zenta village, Aqra district, Kurdistan region, Iraq, Iraqi Bulletin of Geology and Mining, 4(2): 1-15.

Barzani, A.T., Al-Qayim, B.A., 2019. Dolomitization and porosity evaluation of Khurmala, Gara anticline, Dohuk area, Kurdistan Region, Iraq. Iraqi Geological Journal, 52(2), 1-17.

Bassi, D., Posenato, R. and Nebelsick, J. H., 2015. Paleoecological dynamics of shallow-water bivalve carpets from a Lower Jurassic lagoonal setting, northeast Italy, October Palaios, 30 (10),758-770.

Bathurst, R. G. C., 1971. Carbonate sediments and their diagenesis, developments in sedimentology 12: Amsterdam, Elsevier, 620.

Bellen R.C. van, Dunnington H.V., Wetzel R. and Morton D.M., 1959. Iraq. - Lexique Stratigraphique International, Paris, vol. III, Asie, Fascicule 10a.

Bellen, R.C. Van., 1953. Interior report on samples between 4370 - 4965 feet of Kor Mor l 2. NOC library, Kirkuk. GR-207/15.

Berggren, W. A. and Norris, R. D., 1997.Taxonomy and biostratigraphy of (sub) tropical Paleocene planktonic foraminifera. Micropaleontology ,1 (43),1 - 116.

Berggren, W. A. and Pearson, P. N., 2005. A revised tropical to subtropical planktonic foraminiferal zonation of the Eocene and Oligocene: Journal of foraminiferal Research, Vol. 35, 279 – 298.

Berggren, W., Ouda, K., 2003. Upper Paleocene-lower Eocene planktonic foraminiferal biostratigraphy of the Qreiya (Gebel Abu Had) section, Upper Nile Valley (Egypt). Micropaleontology 49 supplements No. 1, p. 105-122.

Berggren, W.A., Kent, D. V., Swisher, I. C. and Aubry, M. P., 1995. A revised geochronology and chronostratigraphy. In, W.A. Berggren, D.V. Kent, M. P. Aubry and J. Hardenbol (Eds.), Geochronology, Time Scales and Global Stratigraphic Correlation. Society of Economic Paleontologists and Mineralogists Special Publication, 54,129-212.

Boersma and Terwindt, 1981. Neap–spring tide sequences of intertidal shoal deposits in a mesotidal estuary. Sedimentology, Vol. 28 Issu. 2, 151-170

Bolle, M. P., Adatte, T., 2001. Palaeocene–early Eocene climatic evolution in the Tethyan realm: clay mineral evidence. Clay Minerals 36, 249–261.

Bolle, M. P., Tantawy, A. A., Pardo, A., Adatte, T., Burns, S., Kassab, A,. 2000. Climatic and environmental changes documented in the upper Paleocene to lower Eocene of Egypt. Eclogae Geologicae Helvetiae, 93, 33–51 pp.

Bourrouilh-Le Jan, F.G., 1979. Hurricanes and rainfalls: a key for dolomitization in the Tidal Flats of western Andros, Bahamas. Abstr., S.E.P.M. Research Symposium. SEPM-AAPG Round table,Houston, p. 423

Bristow, T. F., M.J., Kennedy, K. D., Morrison. and D. D., Mrofka., 2012. The influence of579 authigenic clay formation on the mineralogy and stable isotopic record of lacustrine580 carbonates. Geochimica et Cosmochimica Acta, 90, 64-82.

Chen, J., Chough, S.K., Han, Z. and Lee, J.-H., 2011. An extensive erosion surface of a strongly deformed limestone bed in the Gushan and Chaomidian Formations (late Middle Cambrian to Furongian), Shandong Province, China: Sequence-stratigraphic implications: Sedimentary Geology, v. 233, p. 129–149, doi: 10 .1016 /j. sedgeo .2010.11.002.

Di Stefano, P. and Ruberti, D., 2000. Cenomanian rudist-dominated shelf-margin limestones from the Panormide carbonate platform (Sicily, Italy): facies analysis and sequence stratigraphy. Facies 42, 133–60.

Dianto, A., Subehi, L., Ridwansyah, I. and Hantoro, W., 2019. Clay minerals in the sediments as useful paleoclimate proxy: Lake Sentarum case study, West Kalimantan, Indonesia. IOP Conference Series: Earth and Environmental Science, 311, 12-36.

Do Campo, M., Bauluz, B., Del Papa, C., White, T., Yuste, A., Mayayo, M.J., 2018. Evidence of cyclic climatic changes recorded in clay mineral assemblages from a continental Paleocene-Eocene sequence, northwestern Argentina. Sediment Geol., 368, 44–57

Dumas, S., Arnott, R.W.C., Southard, J.B., 2005. Experiments on oscillatory-flow and combined-flow bed forms; implications for interpreting parts of the shallow-marine sedimentary record. J. Sediment. Res. 75 (3), 501–513.

Dunham, R. J., 1962. Classification of carbonate rocks according to depositional texture. In: Ham, W. E. (ed.), Classification of carbonate rocks: American Association of Petroleum Geologists Memoir, p. 108-121.

Einsele, G., 2000. Sedimentary basins. Evolution, facies, and sediment budget, 2nd edn. Springer, Germany, p 792

El-Nady, H., 2005. The impact of Paleocene/ Eocene (P/E) boundary events in northern Sinai, Egypt: Planktonic foraminiferal biostratigraphy and faunal turnovers, Revue de Paléobiologie, Genève, Vol.24, No.1, p. 1 – 16.

Embry, A. F., Klovan, J. E., 1971. A late Devonian reef tract on northeastern Banks Island. N.W.T. – Bull. Canadian Petrol. Geol., 19, 730-781

Eren, M.; Tasli, K. and Toul, N., 2002. Sedimentology of Liassic carbonates (Pirencik Tepe measured sections) in the Aydinick (Icel) area, Southern Turkey. Journal of Asian earth sciences, 20, 791-801.

Flugel, E., 2004. Microfacies of carbonate rocks, analysis, interpretation and application, Springer, Berlin, 976 p.

Flugel, E., 2010. Microfacies of Carbonate Rocks, 2nd ed. Springer-Verlag Berlin, Germany. 976 pp

Hallock, P. and Glenn, E.C., 1986. Larger foraminfera: Atoll for Paleoenvironmental analysis of Cenozoic Carbonate Depositional Facies, The society of Economic palaeontologists. Minerologists. U.S., Vol.1, p. 55 – 64.

Harding, I. C., Charles, A. J., Marshall, J. E. A., Pälike, H., Roberts, A. P., Wilson, P. A., Jarvis, E., Thorne, R., Morris, E., Moremon, R., Pearce, R. B., Akbari, S., 2011. Sea-level and salinity fluctuations during the Paleocene–Eocene thermal maximum in Arctic Spitsbergen, Earth and planetary Science Letters, 303, 97-107.

Jassim, S. Z. and Buday, T., 2006. Middle Paleocene-Eocene Megasequence (AP 10). In Jassim, S. Z. and Goff, J. C. (Eds)Geology of Iraq. Dolin, Prague and Moravian Museum, Brno, Czech Republic. 155-167.

Jassim, S. Z. and Goff, J. C., 2006. (Eds)Geology of Iraq. Dolin, Prague and Moravian Museum, Brno,Czech Republic. 155-167.

Jiang, J., Hu., X., Garzanti, E., Li, J., Bou Dagher-Fadel, M.K., Sun, G., Xu, Y., 2022.Enhanced storm-induced turbiditic events during early Paleogene hyperthermals (Arabian continental margin, SW Iran). Glob. Planet. Chang. 214, 103832.

Karim, Ch. A., 2009. Stratigraphical and Paleontological Study of Khurmala Formation (Paleocene – Lower Eocene) in Shaqlawa Area -Northern Iraq. Unpublished MSc. Thesis, Mosul University, Iraq, 103.

Kemp, S.J., Ellis, M.A., Mounteney, I., Kender, S., 2016. Palaeoclimatic implications of high-resolution clay mineral assemblages preceding and across the onset of the Palaeocene–Eocene Thermal Maximum, North Sea Basin. Clay Miner., 51, 793–913.

Kidwell, S.M., 1991. Condensed deposits in siliciclastic sequences: observed and expected features. In: Einsele, G., Ricken, W., Seilacher, A. (Eds.), Cycles and Events in Stratigraphy. Springer, Berlin, pp. 682-695.

Mackenzie *et al.*, 2008. Mineral. Mag.72, 329-332. Arvidsonet al. ,2011. Aquat. Geochim.17, 735-747

Malak, Z. A., 2011. Sedimentological and stratigraphical study of the Paleocene – Eocene successions from selected areas – North Iraq. Un published Ph.D. Thesis, Mosul University, 212 p.

Markello, J. and Read, J. F., 1981. Carbonate ramp-to-deeper shale shelf transitions of an Upper Cambrian intrashelf basin, Nolichucky Formation, Southwest Virginia Appalachians, sedimentology, 28, pp. 573-597).

Mutti E., Rosell J., Allen G.P, Fonnesu F. and Sgavetti M., 1985. The Eocene Baronia tide dominated delta-shelf system in the Ager Basin. In: Mila M. and Rosell, J. (eds.) 6th IAS European Regional Meeting, Field Trip Guidebook, 579-600.

Mutti, E., Allen, G.P. and Rosell, J., 1984. Sigmoidal-cross stratification and sigmoidal bars: depositional features diagnostic of tidal sandstones. 5th IAS European Regional Meeting, Marsiglia, Abstract volume, 312-313.

Myrow, P. M., Chen, J., Snyder, Z., Leslie, S., Fike, D. A., Fanning, M., Yuan, J. and Tang, P., 2015. Depositional history, tectonics, and provenance of the Cambrian Ordovician boundary interval in the western margin of the North China block. Bulletin of the Geological Society of America. 127(9-10). 1174-1193. https://doi.org/10.1130/B31228.1

Myrow, P.M. and Southard, J.B., 1996. Tempestite deposition. J. Sed. Res., 66, 875–887.

Myrow, P.M., Southard, J.B., 1991. Combined-flow model for vertical stratification sequences in shallow marine storm-deposited beds. J. Sed. Res. 61 (2), 202–210

Myrow, P.M., Taylor, J.F., Runkel, A.C. and Ripperdan, R.L., 2012. Mixed siliciclastic-carbonate upward deepening cycles of the Upper Cambrian inner detrital belt of Laurentia: Journal of Sedimentary Research, v. 82, p. 216–231, doi: 10 .2110 /jsr .2012 .20

Orabi, H. O. and Hassan, H. F., 2015. Foraminifera from Paleocene early Eocene rocks of Bir El Markha section (West Central Sinai), Egypt: Paleobathymetric and paleotemperature significance. Journal of African Earth Sciences 111, 202-213.

Potter, P.E., Maynard, J.B. and Depetris, P.J., 2005. Mud and Mudstones: Introduction and Overview: Berlin, Heidelberg, Springer-Verlag Berlin Heidelberg, 297 s.p.

Randazzo, A. F. and Zachos, L. G., 1984. Classification and description of dolomite fabrics of rocks from the Floridian aquifer. Sedimentary Geology, 37, 151 – 162.

Röhl, U., Westerhold, T., Bralower, T. J., Zachos, J. C., 2007. On the duration the Paleocene–Eocene Thermal Maximum (PETM), Geochemistry, Geophysics, Geosystems 8.

Salih, A. L. M., 2013. Sedimentology of Sinjar and Khurmala formations (Paleocene-lower Eocene) in Northern Iraq. Unpublished Ph.D. Thesis. University of Baghdad, 175 P.

Salih, N. M., 2010. Stratigraphy and paleoenvironment of the Khurmala and Sinjar Formations at Shira Swar, Shinawa and Bekhme in Kurdistan Region, Northeastern Iraq. Unpublished M.Sc. Thesis. Erbil, University of Salahaddin-Erbil, 157.

Sharma, K.M. and Patnaik, R., 2010. Coprolites from the lower Miocene beds of Baripada. Curr. Sci., v.99(6), pp.804-808.

Sharma, K.M. and Patnaik, R., 2013a. Record of a late Miocene suid, Tetraconodon intermedius from the Baripada beds (Mayurbhanj, Orissa): Age implications. Jour. Palaeontol. Soc. India, v.58(2), pp.213-218.

Sharma, K.M. and Patnaik, R., 2013b. Additional Fossil Batoids (Skates and Rays) from the Miocene Deposits of Baripada Beds, Mayurbhanj District,Orissa, India. Earth Sci. India, v.6(IV), pp.160-184.

Tateo, F., 2020. Clay minerals at the Paleocene–Eocene Thermal Maximum: interpretations, limits, and perspectives. Minerals, 10, 1073.

Tinterri R., 2011. Combined flow sedimentary structures and the genetic link between sigmoidal- and hummocky-cross stratification. GeoActa,10, 43-85, Bologna.

Tucker, M., Wright, V.P. and Dickson, J. A. D., 1990. Carbonate sedimentology. Blackwell Publishing Company, Oxford, Great Britain, pp.10-11.

Wilson, J. L., 1975. Carbonate Facies in Geologic History. Springer Verlag, Berlin. 471p.

Wu, H. G., Zhou, J. J., Hu, W. X., Sun, F. N., Kang, X., Zhang, Y. F., *et al.,* 2022. Origin of authigenic albite in a lacustrine mixed-deposition sequence (Lucaogou Formation, Junggar Basin) and its diagenesis implications. *Energy explor. Exploit.* 40 (1), 132–154. DOI: 10.1177/01445987211042702

Zachos, J. C., Lohmann, K. C., Walker, J. C. G., Wise, S. W., 1993. Abrupt Climate Change and Transient Climates during the Paleogene: A Marine Perspective. The Journal of Geology 101(2):191-213, DOI: 10.1086/648216

Zamagni J., Mutti M., Ballato P., Košir A., 2012. The Paleocene-Eocene thermal maximum (PETM) in shallow-marine successions of the Adriatic carbonate platform (SW Slovenia). Bulletin 124(7–8): 1071–1086.

Zeebe, R. E. and Lourens, L. J., 2019. Solar System chaos and the Paleocene–Eocene boundary age constrained by geology and astronomy. Science 365: 926–929.

Zhang, W., Yang, H., Xie, L., Yang, Y., 2010. Lake-bottom hydrothermal activities and their influence on high-quality source rock development: A case from Chang 7 source rocks in Ordos Basin. Petrol. Etrol. Explor. Dev., 37, 424–429.

Zili, L., Zaghbib-Turki, D., Alegret, L., Arenillas I., Molina, E., 2009. Foraminiferal turnover across the Paleocene/Eocene boundary at the Zumaya section, Spain: record of a bathyal gradual mass extinction: Revista Mexicana de Ciencias Geológicas, v. 26, núm. 3, p. 729-744

Znad, R. K., Aljumaily, I. S. I., 2019. The Impact of Tectonic Setting on Distribution of Kolosh Formation during Paleocene –Lower Eocene in Northern Iraq, Iraqi National Journal of Earth Sciences Vol. 19, No.1, pp. 22-34